

Journal of Organometallic Chemistry, 111 (1976) 197–213
© Elsevier Sequoia S.A., Lausanne — Printed in The Netherlands

A MOLECULAR-ORBITAL STUDY OF THE GROUND AND EXCITED-STATE PROPERTIES OF METALLOCENES OF THE FIRST-ROW TRANSITION-METAL IONS. I

DAVID R. ARMSTRONG, ROBERT FORTUNE and PETER G. PERKINS *

*Department of Pure and Applied Chemistry, University of Strathclyde, Glasgow G1 1XL
(Great Britain)*

(Received October 29th, 1975)

Summary

The CNDO-MO formalism has been used to study the ground- and excited-state properties of unsubstituted metallocenes of the first-row transition-metal ions. The multi-electron configuration interaction (MECI) method has been applied to the calculation of both photo-electron and absorption spectra and the agreement with experiment is satisfactory. The electronic properties of the metallocene series are described and the variations in the bonding schemes within the series are rationalised.

Introduction

The novel bonding patterns characteristic of metal sandwich compounds provide an intriguing challenge to the versatility of current theoretical techniques. The electron-deficient nature of these species, as exemplified by the metallocenes, is best described by molecular-orbital theory and, accordingly, numerous MO methods of varying sophistication have been used to study their ground-state electronic structures [1–11]. However, particular attention has been focussed on ferrocene itself, and no single computational framework has been applied to a wide range of metallocenes. Also, while the excited-state properties of the d^n metallocenes have been partially elucidated within the multi-parameter ligand-field model [12–17], comparable MO calculations of a more general and definitive nature have been limited to the closed-shell molecule ferrocene and its derivatives. It is, therefore, the purpose of this work to attempt a general theoretical interpretation of both ground- and excited-state properties of the metallocenes and to correlate the results with the available experimental data.

Method, results, and discussion

A. General

A staggered D_{5d} molecular geometry was assumed for all the metallocenes studied. The metal-carbon bond lengths are listed in Table 1, while the geometry of the cyclopentadienyl (Cp) ring was as in ref. 18.

All ground-state calculations were carried out within a modified [19] CNDO computational framework [20] incorporating a generalisation of Dewar's half-electron method [21] and the MECI * method [22].

One modification to the basic CNDO equations used here is the implementation of the Wolfsberg-Helmholtz approximation [23] to determine the values of the off-diagonal Fock-matrix elements. We carried out preliminary studies in order to determine an appropriate value for the Wolfsberg-Helmholtz proportionality constant k . Vanadocene was chosen for this purpose and calculations were performed over a range of k values from 1.0 to 2.0. The variation of molecular orbital energies with k is shown in Fig. 1.

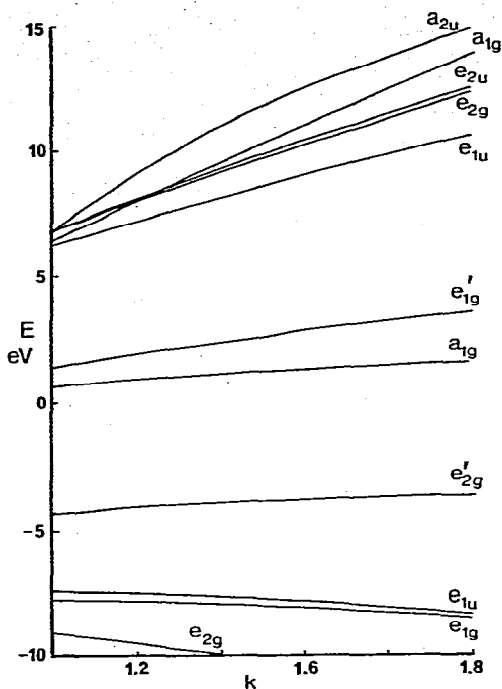
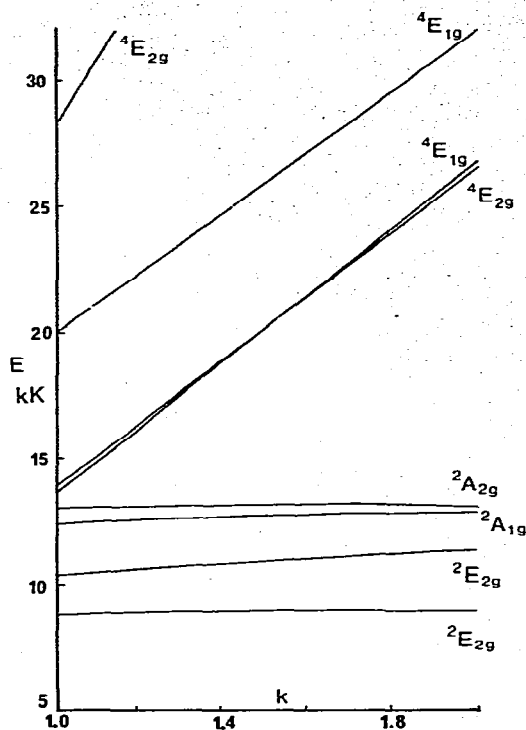
For all values chosen, the outer molecular-orbital sequence of vanadocene is found to be $(e_{2g})^4(e_{1g})^4(e_{1u})^4(e'_{2g})^3(a_{1g})^0(e'_{1g})^0$, the half-electron SCF procedure placing 0.75 electrons of α -spin and 0.75 electrons of β -spin in each of the highest filled (e'_{2g}) molecular orbitals. The MECI calculations consistently predict a ${}^4A_{2g}$ ground state (arising from the high-spin outer electronic configuration $(e'_{2g})^2(a_{1g})^1$ over this range of k values. Use of the Racah parameters B and C , evaluated for the metal ion in its zeroth oxidation state [24], as perturbations in the MECI process results in the excited states depicted graphically in Fig. 2. Inspection of Fig. 2 (a Tanabe-Sugano-type [25] diagram) clearly indicates the optimum value of 1.4 for k , which gives the best agreement between calculated and experimental optical absorption spectra (Table 2). Consequently, in initial studies of the metallocene series, a k value of 1.4 was adopted: the ground-state properties derived from this series of calculations are summarised in Tables 3 and 4.

TABLE 1
MOLECULAR GEOMETRIES

Complex	Metal-carbon bond length (nm)	Ref.
$V(Cp)_2^{2+}$	0.205 ^a	
$V(Cp)_2^+$	0.219 ^a	
$V(Cp)_2$	0.230	41
$Cr(Cp)_2^+$	0.202 ^a	
$Cr(Cp)_2$	0.222	42
$Mn(Cp)_2$	0.238	43
$Fe(Cp)_2^+$	0.196 ^a	
$Fe(Cp)_2$	0.2056	18
$Co(Cp)_2^+$	0.204 ^a	
$Co(Cp)_2$	0.213	41
$Ni(Cp)_2$	0.2196	44

^a Estimated.

* MECI = multi-electron configuration interaction.

Fig. 1. Variation of eigenvalues with k in $V(Cp)_2$.Fig. 2. Tanabe-Sugano-type diagram for $V(Cp)_2$.

The accepted bonding patterns are correctly reproduced by the method used here, the outer molecular orbital sequence being in general, $e'_{1g} > a_{1g} > e_{2g}$. The experimental estimate [26] of 0.91 for the metal d_z^2 orbital coefficient of the a_{1g} molecular orbital in the ferrocenium cation is in satisfactory agreement with the calculated value of 0.99. Electron density contour maps are shown in Fig. 3 for ferrocene.

The calculated metal-carbon bond indices provide a quantitative measure of the degree of metal-ring interaction and on this basis, the metal-ligand interac-

TABLE 2

CALCULATED AND EXPERIMENTAL ABSORPTION SPECTRUM OF $V(Cp)_2$, $k = 1.4$

E calcd. (kK)	E exp. (kK)	Assignment
18.8	17.6	${}^4A_{2g} \rightarrow {}^4E_{1g}$
18.9	19.7	${}^4E_{2g}$
24.7	24.6	${}^4E_{1g}$
8.8	—	${}^2E_{2g}$
10.8	—	${}^2E_{2g}$
12.6	—	${}^2A_{1g}$
13.1	—	${}^2A_{2g}$

TABLE 3
METALLOCENE GROUND-STATE ELECTRONIC PROPERTIES ($k = 1.4$)

Complex	Atom charges		Bond Indices		Metal atomic orbital occupancies		
	M	C	M—C	C—C	s	p	d
V(Cp) ₂ ²⁺	+0.846	+0.003	0.356	1.268	0.311	0.811	3.032
V(Cp) ₂ ⁺	+0.264	+0.003	0.339	1.286	0.313	0.808	3.615
V(Cp) ₂	-0.281	-0.004	0.312	1.302	0.307	0.779	4.195
Cr(Cp) ₂ ⁺	-0.231	+0.047	0.349	1.257	0.305	0.762	5.165
Cr(Cp) ₂	-0.599	+0.026	0.338	1.285	0.309	0.748	5.543
Mn(Cp) ₂	-0.193	-0.006	0.323	1.293	0.323	0.844	6.026
Fe(Cp) ₂ ⁺	-0.416	+0.072	0.368	1.242	0.311	0.835	7.271
Fe(Cp) ₂	-0.610	+0.034	0.357	1.270	0.318	0.818	7.474
Co(Cp) ₂ ⁺	-0.421	+0.076	0.381	1.239	0.324	0.875	8.222
Co(Cp) ₂	-0.499	+0.027	0.292	1.271	0.320	0.849	8.328
Ni(Cp) ₂	-0.412	+0.021	0.229	1.272	0.310	0.845	9.257

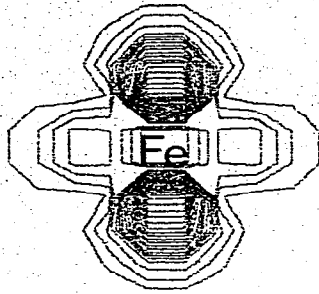
tion is found to increase in the order: Ni(Cp)₂ < Co(Cp)₂ < V(Cp)₂ < Mn(Cp)₂ < Cr(Cp)₂ < Fe(Cp)₂. This is in agreement with the limited experimental data available [14,27-29]. The predicted ground states are obviously compatible, in general, with experiment [30].

It is possible to repeat the SCF process for the unipositive molecular ion (assuming the same molecular geometry) and to obtain the ground and excited states of the ionised species by means of a MECI calculation. Such calculations were therefore carried out on the molecular ions, M(Cp)₂⁺, resulting from removal of an electron from the parent metallocenes. Only the lowest-energy molecular ionisation potentials will be considered explicitly.

For comparison, the molecular-orbital energies have been plotted for the neutral metallocenes (Fig. 4) and their ions (Fig. 5). For the highest e_{1g} (e'_{1g}) and a_{1g} levels, the energy variation is somewhat erratic and is due to the increasing number of valence electrons on crossing the transition series from vanadium to

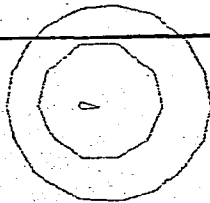
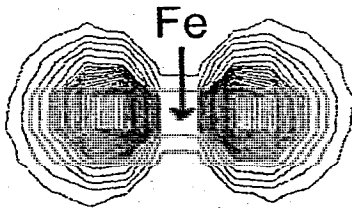
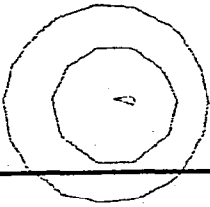
TABLE 4
GROUND-STATE ELECTRONIC STRUCTURES OF d^1-d^8 METALLOCENES

	Predicted ground state and electronic configuration				Experimental ground state
	e'_{2g}	a_{1g}	e'_{1g}		
V(Cp) ₂ ²⁺	1	0	0	² E _{2g}	Jahn-Teller distortion
V(Cp) ₂ ⁺	1	1	0	³ E _{2g}	³ A _{2g}
V(Cp) ₂	2	1	0	⁴ A _{2g}	⁴ A _{2g}
Cr(Cp) ₂ ⁺	2	1	0	⁴ A _{2g}	⁴ A _{2g}
Cr(Cp) ₂	2	2	0	³ A _{2g}	³ A _{2g}
Mn(Cp) ₂	3	2	0	² E _{2g}	⁶ A _{1g}
Fe(Cp) ₂ ⁺	3	2	0	² E _{2g}	² E _{2g}
Fe(Cp) ₂	4	2	0	¹ A _{1g}	¹ A _{1g}
Co(Cp) ₂ ⁺	4	2	0	¹ A _{1g}	¹ A _{1g}
Co(Cp) ₂	4	2	1	² E _{1g}	² E _{1g}
Ni(Cp) ₂	4 (e_{1g})	2	2	³ A _{2g}	³ A _{2g}



(a)

Fig. 3(a)



(b)

Fig. 3(b)

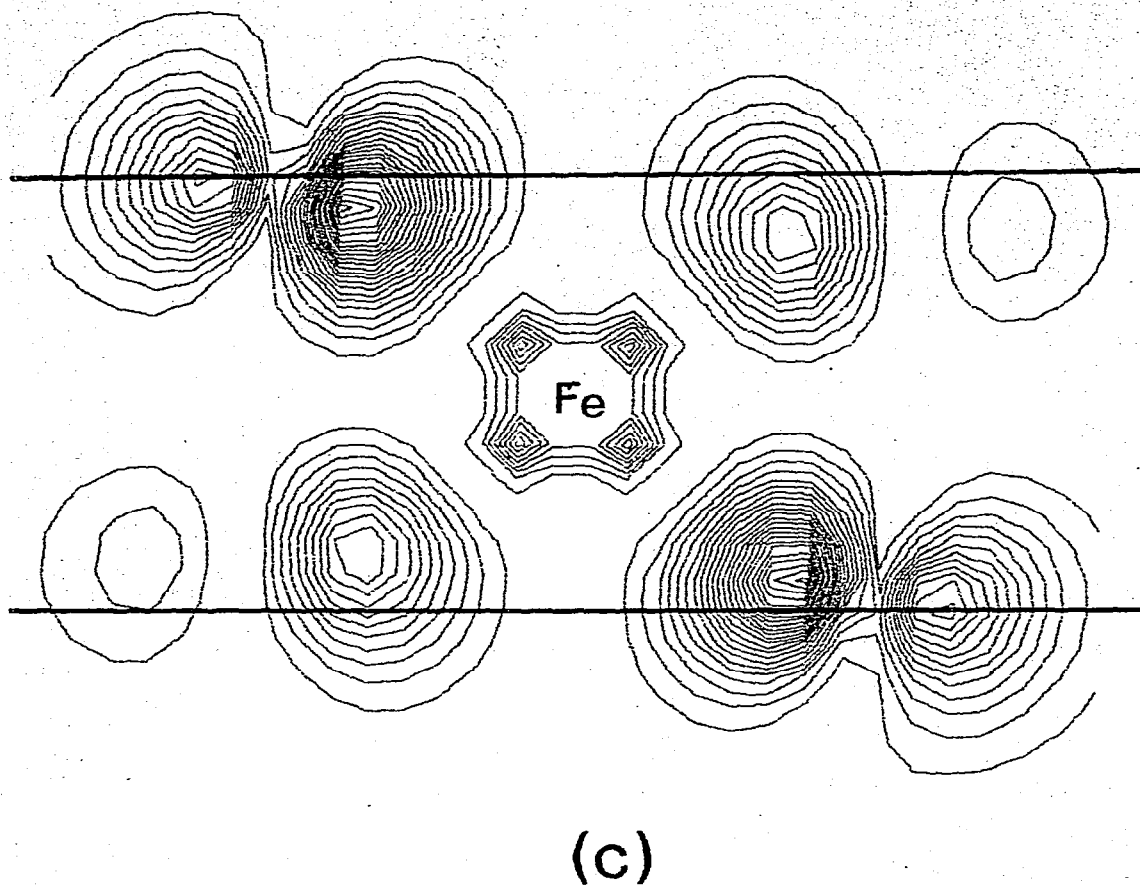


Fig. 3(c)

nickel. For all the neutral metallocenes studied with the exception of nickelocene, the outer molecular orbital sequence is $e'_{2g} < a_{1g} < e'_{1g}$. This is consistent with the majority of previous calculations. Many of the molecular orbitals are strongly metal-localised; the degree of localisation is well shown in Table 5.

The lower-energy ionisation potentials, as evaluated from MECI calculations on both $M(\text{Cp})_2$ and $M(\text{Cp})_2^+$, are summarised in Table 6. These results will now be discussed further in relation to the individual metallocenes. Unless otherwise stated, all photo-electron spectral data have been abstracted from ref. 31.

B. Electronic ground states of the metallocene series

Vanadocene is predicted to have the outer electronic configuration $(e'_{2g})^2(a_{1g})^1(e'_{1g})^0$ corresponding to the high-spin $^4A_{2g}$ ground state: this agrees with both previous calculations [10,11] and experiment [14,32]. Removal of an electron from the e'_{2g} or a_{1g} levels gives the $^3E_{2g}(e'_{2g})^1(a_{1g})^1$ and $^3A_{2g}(e'_{2g})^2$ states, respectively, and these ionisations are calculated to require 6.9 and 7.5 eV. Experimentally, a low-energy band in the photoelectron spectrum at 6.78 eV has been attributed to a superposition of these energetically similar states [31].

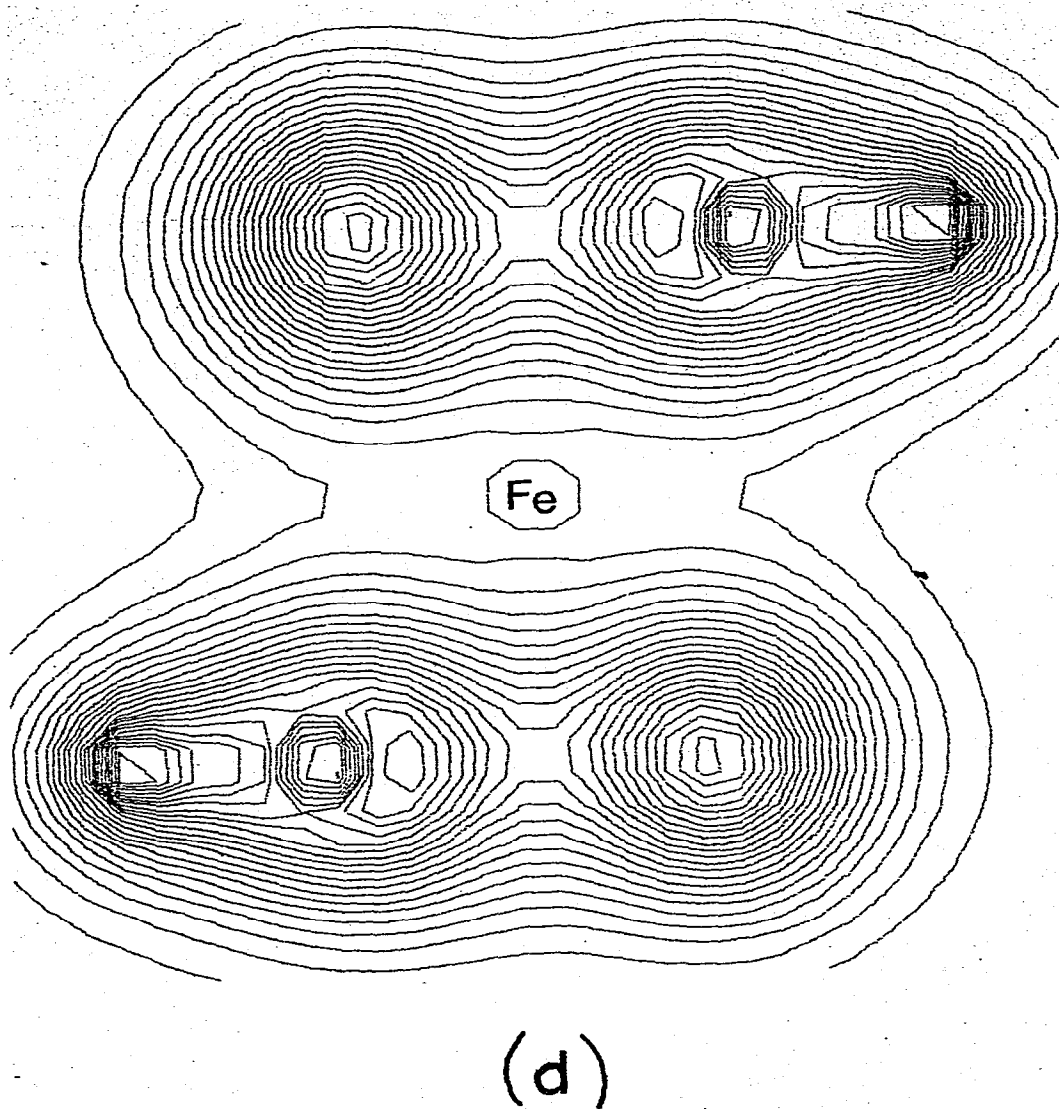


Fig. 3(d)

Fig. 3. Density contours for ferrocene orbitals. Horizontal lines show the position of the ring planes: (a) a_{1g} orbital, (b) e'_{2g} orbital, (c) d_{xz} component of e'_{1g} orbital, (d) total electron density in ferrocene, vertical section.

The calculated ${}^3A_{2g}$ ground state for chromocene will help to resolve the controversy which exists at present over the assignment of the lower-energy photoelectron bands of this compound. The MECI calculation predicts a ${}^4A_{2g}(e_{2g})^2(a_{1g})^1$ ground state for the $\text{Cr}(\text{Cp})_2^+$ ion, as it does also for the d^3 neutral vanadocene, with the higher-energy states quoted in Table 6.

For manganocene a ${}^2E_{2g}$ ground state corresponding to the outer electronic configuration $(e'_{2g})^3(a_{1g})^2$ is predicted, identical to that of the isoelectronic fer-

(continued on p. 206)

TABLE 5
METAL-ORBITAL CONTRIBUTIONS TO HIGHER FILLED AND LOWER EMPTY MOLECULAR ORBITALS

	$a_{2u}^*(d_z)$	$a_{1g}^*(g)$	e_{2g}^*	$e_{1u}^*(d_x d_y)$	$e_{1g}^*(d_{xz}, d_{yz})$	$a_{1g}^*(d_{z^2})$	$e_{2g}^*(d_{x^2-y^2}, d_{xy})$	e_{1u}	e_{1g}
V(Cp) ₂	0.801	0.805	0.010	0.848	0.699	0.978	0.980	0.028	0.193
V(Cp) ₂ ⁺	0.830	0.810	0.001	0.837	0.627	0.978	0.980	0.032	0.220
Cr(Cp) ₂	0.783	0.780	0.001	0.839	0.607	0.980	0.970	0.025	0.229
Cr(Cp) ₂ ⁺	0.797	0.797	0.009	0.834	0.514	0.980	0.966	0.028	0.245
Mn(Cp) ₂	0.651	0.817	0.002	0.824	0.740	0.990	0.992	0.063	0.225
Mn(Cp) ₂ ⁺	0.726	0.817	0.002	0.812	0.581	0.990	0.988	0.073	0.359
Fe(Cp) ₂	0.386	0.651	0.009	0.656	0.518	0.990	0.958	0.038	0.282
Fe(Cp) ₂ ⁺	0.537	0.724	0.007	0.712	0.465	0.990	0.953	0.043	0.362
Co(Cp) ₂	0.329	0.752	0.004	0.659	0.548	0.992	0.978	0.061	0.375
Co(Cp) ₂ ⁺	0.428	0.799	0.003	0.694	0.472	0.992	0.968	0.069	0.430
Ni(Cp) ₂	0.262	0.808	0.002	0.610	0.365	0.996	0.986	0.076	0.561
Ni(Cp) ₂ ⁺	0.331	0.817	0.002	0.645	0.299	0.996	0.980	0.086	0.607

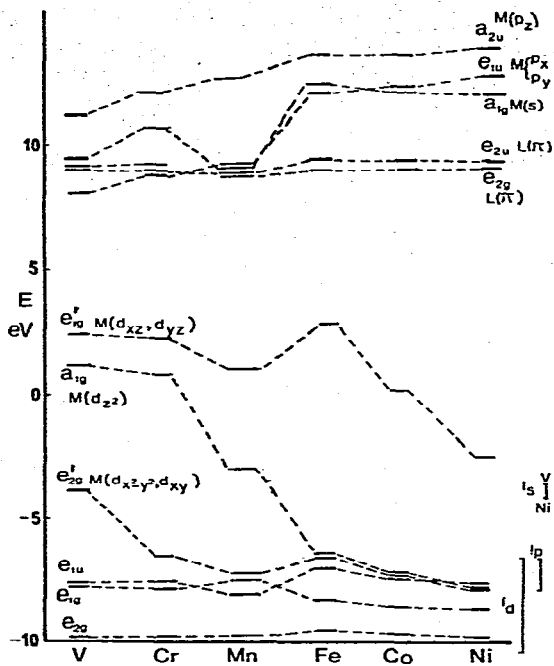


Fig. 4. Variation of eigenvalues of $M(\text{Cp})_2$ for $k = 1.4$.

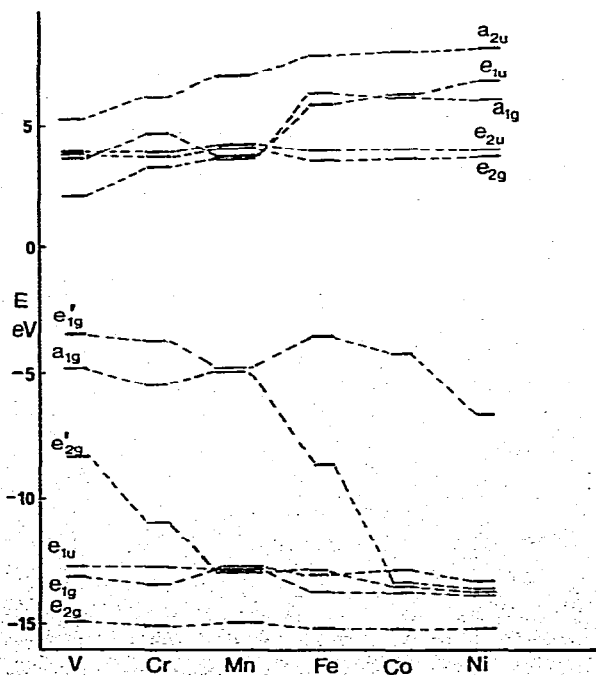


Fig. 5. Variation of eigenvalues of $M(\text{Cp})_2^+$ for $k = 1.4$.

TABLE 6
LOW-ENERGY IONISATION PROCESSES IN THE NEUTRAL METALLOCENES

Complex	M(Cp) ₂			M(Cp) ₂ ⁺			Ionisation Energies (eV)				
	Molecular ground state and outer electronic configuration			Molecular ion states and outer electronic configuration			Calc.	Exp.			
	e' _{2g}	a _{1g}	e' _{1g}	e' _{2g}	a _{1g}	e' _{1g}					
V(Cp) ₂	⁴ A _{2g}	2	1	0	³ E _{2g}	1	1	0	6.9	6.78	
					³ A _{2g}	2	0	0	7.5		
Cr(Cp) ₂	³ A _{2g}	2	2	0	⁴ A _{2g}	2	1	0	7.3	5.71	
					² E _{1g}	2	1	0	8.5		7.04
					² E _{2g}	1	2	0	8.8		7.30
					² A _{2g}	2	1	0	9.1		7.58
					² A _{1g}	2	1	0	9.3		
					² E _{2g}	3	0	0	10.7		
Mn(Cp) ₂	² E _{2g}	3	2	0	³ A _{2g}	2	2	0	7.5	6.26	
					³ E _{2g}	3	1	0	8.3		6.91
					¹ E _{1g}	2	2	0	8.5		
					¹ A _{1g}	4	0	0	9.2		
Co(Cp) ₂	² E _{1g}	4	2	1	¹ A _{1g}	4	2	0	4.3	5.56	
					³ E _{1g}	3	2	1	6.6		
					³ E _{2g}	3	2	1	6.9		7.18
					¹ E _{1g}	3	2	1	7.4		
					¹ E _{2g}	3	2	1	7.5		7.63
					³ E _{1g}	4	1	1	8.5		8.01
Ni(Cp) ₂	³ A _{2g}	4	2	2	² E _{1g}	4	2	1	5.7	6.51	
					⁴ E _{2g}	3	2	2	8.9		

rocenium cation, and for the molecular ion the lowest energy state is found to be ³A_{2g}(e'_{2g})²(a_{1g})². In this instance the e'_{2g} - a_{1g} orbital splitting is significantly reduced in comparison with chromocene. The low-spin ground state of mangano-cene is in agreement with the work of Rabalais et al. [33].

Ferrocene is the only neutral metallocene of the first-row transition metals having a singlet ¹A_{1g} ground state arising from an outer electronic configuration (e'_{2g})⁴(a_{1g})². Since Dewar's method and the closed-shell molecular orbital formalism [34] are now coincident, a critical appraisal of Koopman's theorem [35] is now possible. The calculated and experimental ionisation potentials are listed in Table 7.

Cobaltocene is found to have a ²E_{1g}(e'_{2g})⁴(a_{1g})²(e'_{1g})¹ ground state, in accord with experimental observations [36]. Ionisation from the (e_{1g}) level produces a ¹A_{1g} ground state for the cobaltocenium cation. The higher-energy states, together with assignments, are shown in Table 6 to be essentially in agreement with experiment.

The outer electronic configuration (e_{1g})⁴(a_{1g})²(e'_{1g})², for nickelocene, correctly formulates a ³A_{2g} ground state [37]. Ionisation gives a ²E_{1g} ground state for the molecular ion, also in agreement with experiment.

In order to develop a method by which absorption spectra can be quantita-

TABLE 7
ORBITAL ENERGIES AND I.P.'s (eV) FOR $\text{Fe}(\text{Cp})_2$

I.P. (calcd.)	Assignment	I.P. (exp.) ^a	Assignment
6.7	e_{2g}	6.9	e_2'
6.6	a_{1g}	7.2	a_1'
7.2	e_{1g}	8.7	$e_{1''}$
8.6	e_{1u}	9.1	e_1''

^a Ref. 40.

tively predicted, we must examine the effect of k and other input data on the excited states. Hence, we have constructed Tanabe—Sugano-type diagrams (as in Fig. 2) for selected metallocenes.

C. Excited-state properties of the metallocene series

The ${}^4A_{2g}$ ground state of vanadocene permits three low-energy spin-allowed transitions, as demonstrated in Fig. 2. The low-lying excited-state energies (excluding two-electron excitations which are of negligible intensity) and experimental spectral bands are compared in Table 2. For vanadocene the agreement is very good, as expected from the parametrisation scheme.

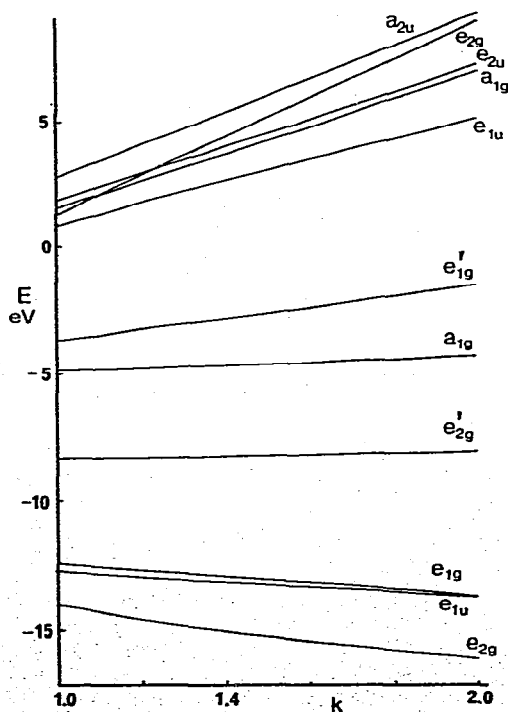


Fig. 6. Variation of eigenvalues with k for $\text{V}(\text{Cp})_2^+$.

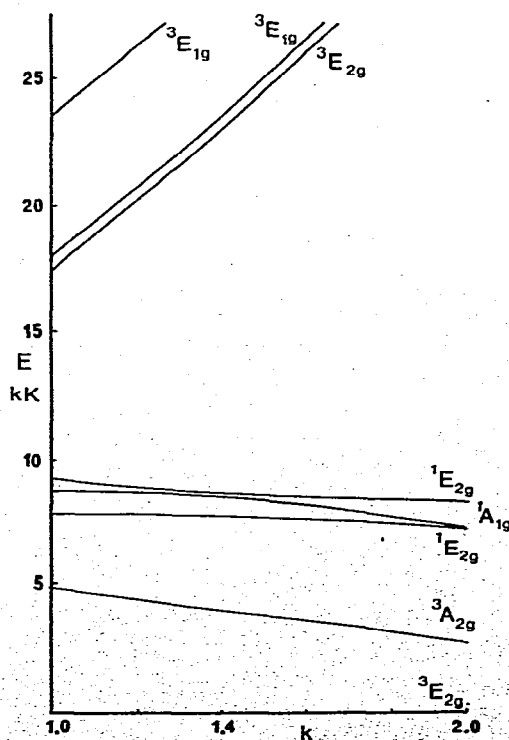


Fig. 7. Tanabe—Sugano-type diagram for $\text{V}(\text{Cp})_2^+$.

The d^2 complex $V(Cp)_2^+$ and the d^1 complex $V(Cp)_2^{2+}$ cannot be regarded as simple ionisation products of the parent vanadocene, since the molecular geometry alters to accommodate the effect of the reduced ionic radii of the vanadium(III) and vanadium(IV) ions. The variation in molecular-orbital energies with k is depicted graphically for $V(Cp)_2^+$ in Fig. 6 and the corresponding Tanabe—Sugano diagram is shown in Fig. 7. Dewar's SCF procedure shows the existence of two possible ground states. These are the ${}^3A_{2g}$ and ${}^3E_{2g}$ states. The MECI calculation shows the latter state to be more stable in the range of k values chosen but indicates the occurrence of the ${}^3A_{2g}$ ground state at higher ligand-field strengths. Magnetic data support a ${}^3A_{2g}$ ground state.

Similar effects are evident for the d^1 complex $V(Cp)_2^{2+}$. The e'_{1g} level is again strongly dependent on ligand-field strength (Fig. 8), resulting in the energy of the ${}^2E_{1g}$ excited state being radically altered as k is increased (Fig. 9). The ground state is found to be the Jahn—Teller susceptible ${}^2E_{2g}$ state and further calculations show that a Jahn—Teller distortion to C_{2v} symmetry leads to the orbital sequence $(d_{x^2-y^2})^1(d_{xy})(d_{yz})(d_{xz})$. This distortion, shown schematically in Fig. 10, is identical to that postulated for formation of protonated ferrocene, $Fe(Cp)_2H^+$, where it was concluded that the metal—ring bonding is essentially unaltered by the degree of distortion [38]. We assumed the vanadium—carbon bond lengths remained unaltered during the distortion and reduced the ring—metal—ring angle from 180° to 165° . It was found that reduction of this angle

(continued on p. 211)

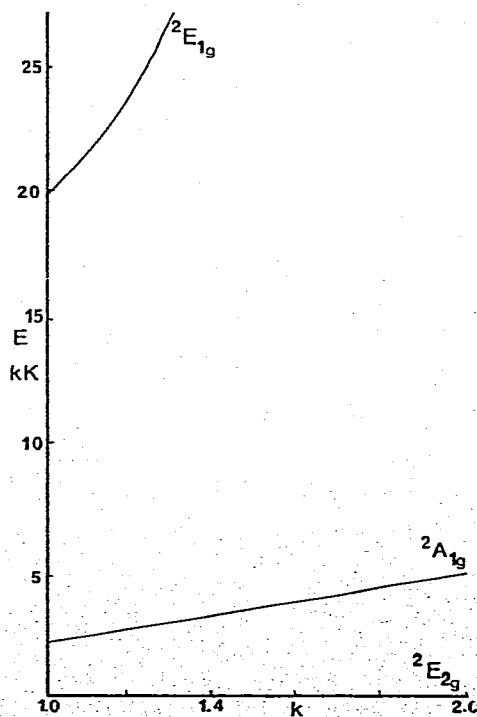
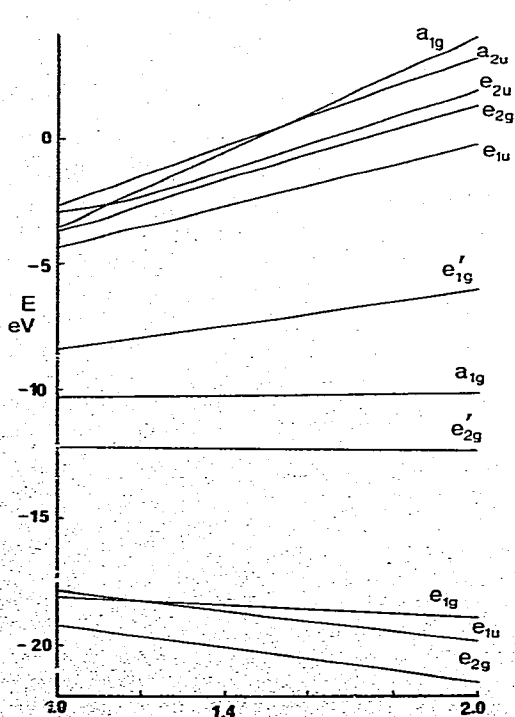
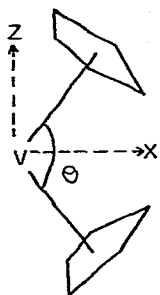
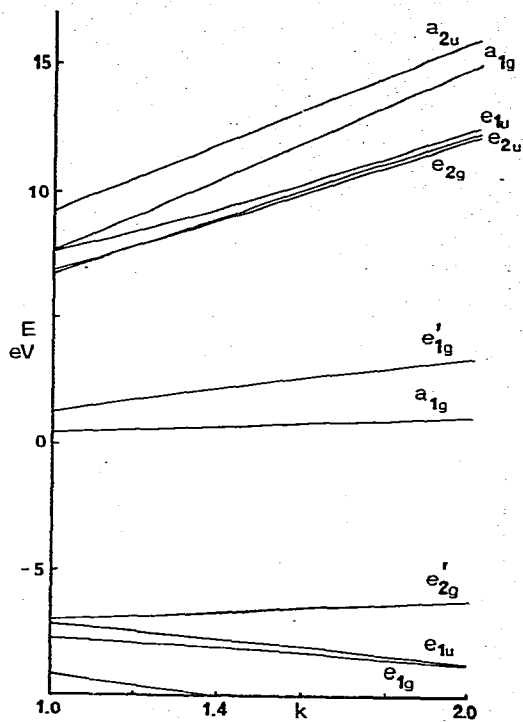
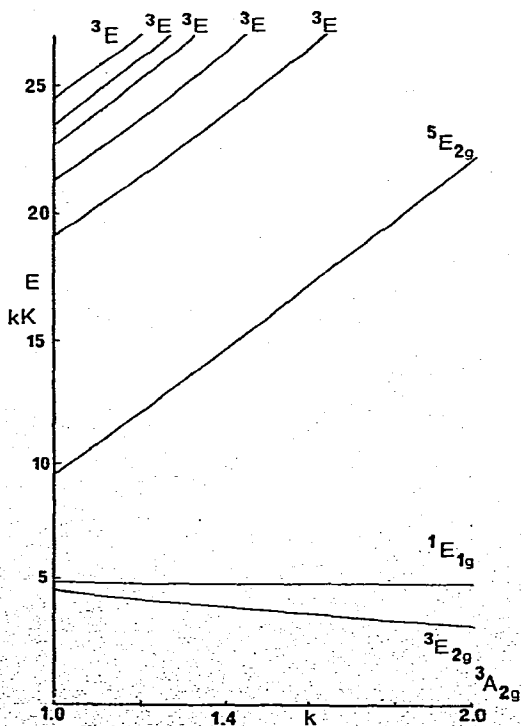
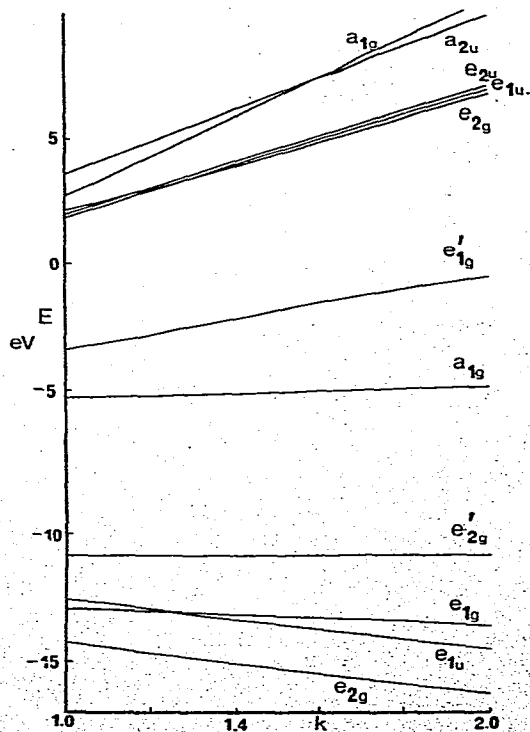


Fig. 8. Variation of eigenvalues with k for $V(Cp)_2^{2+}$. Fig. 9. Tanabe—Sugano-type diagram for $V(Cp)_2^{2+}$.

Fig. 10. C_{2v} distortion of $V(Cp)_2^{2+}$.Fig. 11. Variation of eigenvalues with k for $Cr(Cp)_2$.Fig. 12. Tanabe-Sugano-type diagram for $Cr(Cp)_2$.Fig. 13. Variation of eigenvalues with k for $Cr(Cp)_2^+$.

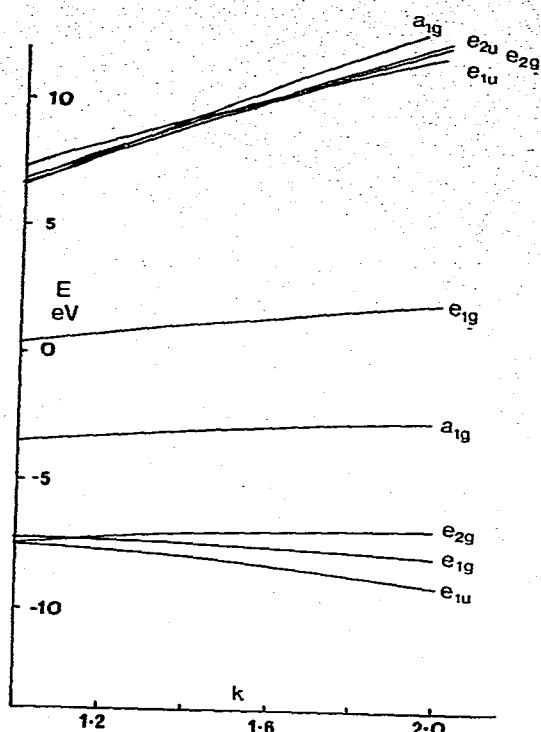
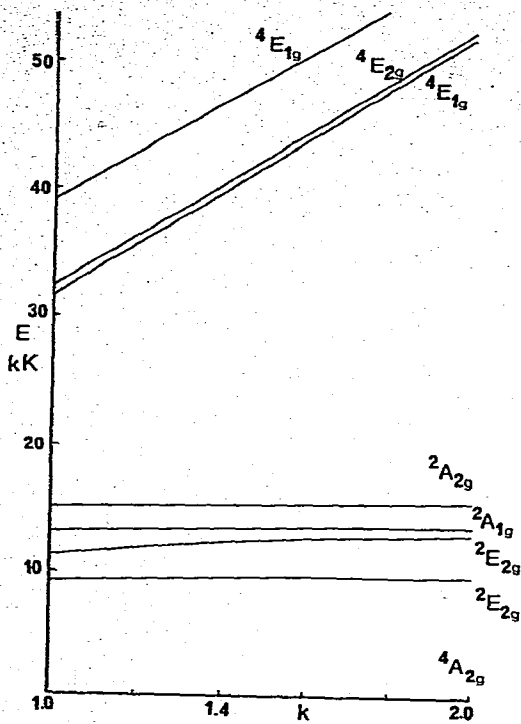


Fig. 14. Tanabe-Sugano-type diagram for $\text{Cr}(\text{Cp})_2^+$. Fig. 15. Variation of eigenvalues with k for $\text{Mn}(\text{Cp})_2$.

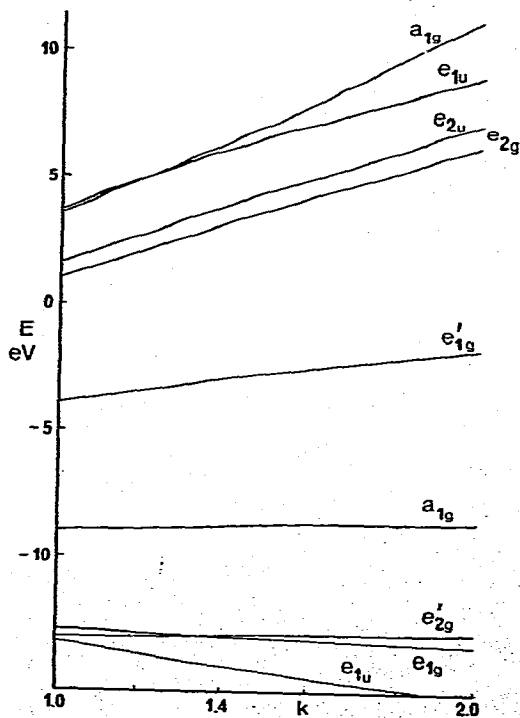
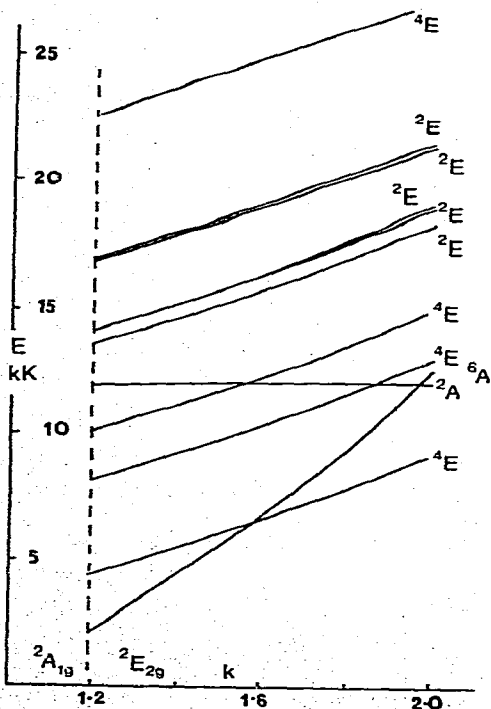


Fig. 16. Tanabe-Sugano-type diagram for $\text{Mn}(\text{Cp})_2$. Fig. 17. Variation of eigenvalues with k for $\text{Fe}(\text{Cp})_2^+$.

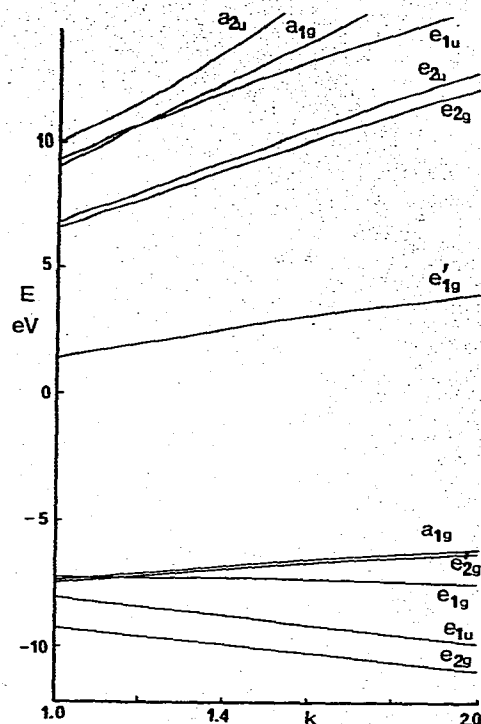
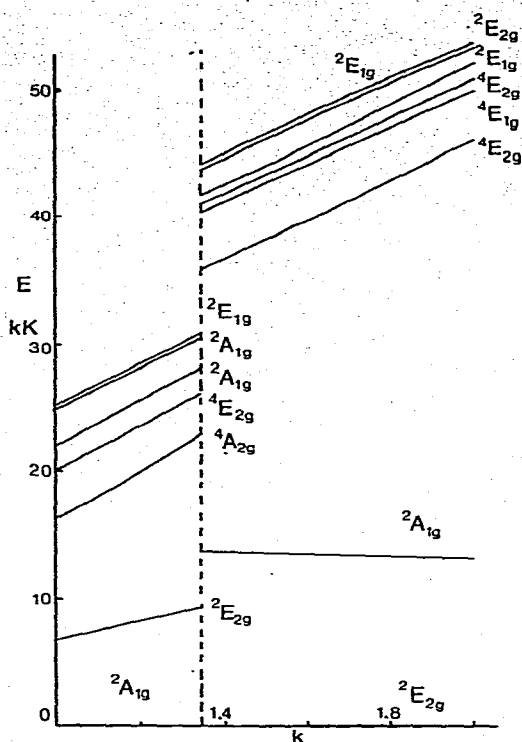


Fig. 18. Tanabe-Sugano-type diagram for $\text{Fe}(\text{Cp})_2^+$. Fig. 19. Variation of eigenvalues with k for $\text{Fe}(\text{Cp})_2^+$.

strengthened the overall metal-ring interaction, thereby stabilising the system; this, however, does not compensate for the increased nuclear energy brought about by mutual approach of the rings. It was next shown, however, that a small increase in metal-carbon bond length (0.01 nm) is sufficient to stabilise the Jahn-Teller distorted system with respect to the unperturbed species and it is therefore concluded that for C_{2v} distortion to occur, a concomitant increase in metal-ligand separation is required. With this restriction, the above model of protonated sandwich compounds is perfectly acceptable. This view is reinforced by the existence of the C_{2v} species $\text{Mo}(\text{Cp})_2\text{H}_2$ [39].

A singlet, triplet or pentuplet ground state can exist for d^4 chromocene. Experimental evidence indicates a ${}^3E_{2g}$ ground state, while the calculations predict a ${}^3A_{2g}$ ground state: the double occupancy of the a_{1g} level merely reemphasises the importance of configuration interaction.

The chromocinium cation has a ${}^4A_{2g}$ ground state like the isoelectronic vanadocene. Consequently, for these species both the molecular-orbital sequence (Fig. 13) and Tanabe-Sugano diagram (Fig. 14) are similar. In $\text{Cr}(\text{Cp})_2^+$, however, although the $e'_{2g} - a_{1g}$ separation is comparable to that in vanadocene, the e'_{1g} level is at considerably higher energy. This results in the spin-allowed excitations being much more energetic than in vanadocene.

Experimental data favour a high-spin ${}^6A_{1g}$ ground state for manganocene,

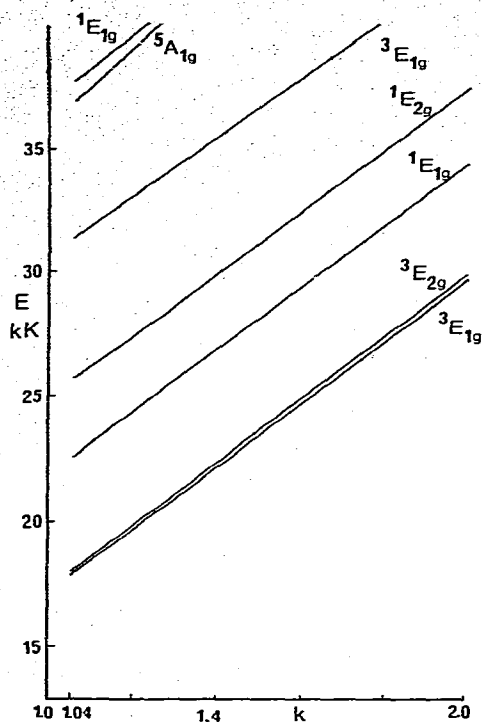


Fig. 20. Tanabe—Sugano-type diagram for $\text{Fe}(\text{Cp})_2$.

while $\text{Fe}(\text{Cp})_2^+$ has been shown to have a ${}^2E_{2g}$ ground state. The eigenvalue variations with k are similar for both species (Figs. 15 and 17) and, consequently, a ${}^2E_{2g}$ ground state is predicted for both. At lower values of k (<1.4), the outer electronic configuration of $\text{Fe}(\text{Cp})_2^+$ leads to a ${}^2A_{1g}$ ground state, whilst for values of $k > 1.4$ the calculated electronic transition energies deviate from experiment. The Tanabe—Sugano diagram for manganocene (Fig. 16) corresponds to that expected for the ferrocenium cation. Similarly for ferrocene itself, for a k value close to 1.0, the Tanabe—Sugano diagram (Fig. 20) gives results in good agreement with experiment. The outer electronic configuration is, however, $(a_{1g})^2(e_{1g})^4(e'_{1g})^0$. At higher ligand-field strengths, however, this order is changed and the generally accepted $(e'_{2g})^4(a_{1g})^2(e'_{1g})^0$ orbital sequence prevails. The associated Tanabe—Sugano diagram (Fig. 20) renders a satisfactory interpretation of the lower-energy ligand-field bands of ferrocene. In the context of these calculations, it should be remembered that the spectral energies involved are rather small.

Acknowledgement

One of us (R.F.) thanks the University of Strathclyde for a Crawford Bursary.

References

- 1 A.D. Liehr and C.J. Ballhausen, *Acta Chem. Scan.*, **11** (1957) 207.
- 2 J.P. Dahl and C.J. Ballhausen, *Kgl. Danske Videnskab, Selskab Mat. Fys. Medd.*, (1961) 33.

- 3 R.D. Fischer, *Theor. Chim. Acta*, 1 (1963) 418.
- 4 A.T. Armstrong, D.G. Carroll and S.P. McGlynn, *J. Chem. Phys.*, 47 (1967) 1104.
- 5 I.H. Hillier and R.M. Canadine, *Disc. Faraday Soc.*, 47 (1969) 27.
- 6 M.M. Coutiere, J. Demuyne and A. Veillard, *Theor. Chim. Acta*, 27 (1972) 281.
- 7 E.J. Baerends and P. Ros, *Chem. Phys. Lett.*, 23 (1973) 391.
- 8 N. Rösch and K.H. Johnson, *Chem. Phys. Lett.*, 24 (1974) 179.
- 9 T. Ziegler, *Acta Chem. Scand.*, A, 28 (1974) 29.
- 10 J.H. Schachtschneider, R. Prins and P. Ros, *Inorg. Chim. Acta*, 1 (1967) 462.
- 11 M.F. Rettig and R.S. Drago, *J. Amer. Chem. Soc.*, 91 (1969) 3432.
- 12 D.R. Scott and F.A. Matsen, *J. Phys. Chem.*, 72 (1963) 16.
- 13 D.R. Scott and R.S. Becker, *J. Organometal. Chem.*, 4 (1965) 409.
- 14 R. Prins and J.D.W. van Voorst, *J. Chem. Phys.*, 49 (1968) 4665.
- 15 Y.S. Sohn, D.N. Hendrickson and H.B. Gray, *J. Amer. Chem. Soc.*, 93 (1971) 3603.
- 16 J.R. Perumareddi, *J. Phys. Chem.*, 71 (1971) 3144.
- 17 K.D. Warren, *J. Phys. Chem.*, 77 (1973) 1681.
- 18 R.K. Böhn and A. Haaland, *J. Organometal. Chem.*, 5 (1966) 470.
- 19 D.R. Armstrong, P.G. Perkins and J.J.P. Stewart, *J. Chem. Soc.*, A, (1971) 3654.
- 20 J.A. Pople, D.P. Santry and G.A. Segal, *J. Chem. Phys.*, 43 (1965) S129.
- 21 M.J.S. Dewar, J.A. Hashmall and C.G. Venier, *J. Amer. Chem. Soc.*, 90 (1968) 1953.
- 22 D.R. Armstrong, R. Fortune, P.G. Perkins and J.J.P. Stewart, *J. Chem. Soc., Faraday Trans. II*, (1972) 1839.
- 23 M. Wolfsberg and L. Helmholtz, *J. Chem. Phys.*, 20 (1952) 837.
- 24 J.S. Griffith, *The Theory of Transition Metal Ions*, Cambridge, 1961.
- 25 Y. Tanabe and S. Sugano, *J. Phys. Soc. Japan*, 9 (1954) 753, 766.
- 26 R. Prins, *Mol. Phys.*, 19 (1970) 603.
- 27 H.P. Fritz, *Adv. Organometal. Chem.*, 1 (1963) 239.
- 28 G. Wilkinson, P.L. Pauson and F.A. Cotton, *J. Amer. Chem. Soc.*, 76 (1954) 1970.
- 29 L. Friedman, A.P. Irsa and G. Wilkinson, *J. Amer. Chem. Soc.*, 77 (1955) 3689.
- 30 D.A. Brown, *Transition Metal Chem.*, 3 (1966) 1.
- 31 S. Evans, M.L.H. Green, B. Jewitt, G.H. King and A.F. Orchard, *J. Chem. Soc., Faraday Trans. II*, (1974) 356.
- 32 R. Prins, P. Biloen and J.D.W. van Voorst, *J. Chem. Phys.*, 46 (1967) 1216.
- 33 J.W. Rabalais, L.O. Werme, T. Bergmark, L. Karlsson, M. Husain and K. Siegbahn, *J. Chem. Phys.*, 57 (1972) 1185.
- 34 C.C.J. Roothaan, *Rev. Mod. Phys.*, 23 (1951) 69.
- 35 T. Koopmans, *Physica*, 1 (1933) 104.
- 36 M. Nussbaum and J. Voitländer, *Z. Naturforsch.*, A, 20 (1965) 1417.
- 37 R. Prins, P. Biloen and J.D.W. van Voorst, *Chem. Phys. Lett.*, 1 (1967) 54.
- 38 C.J. Ballhausen and J.P. Dahl, *Acta Chem. Scand.*, 15 (1961) 1333.
- 39 J.H. Ammeter and J.D. Swalen, *J. Chem. Phys.*, 57 (1972) 478.
- 40 S. Evans, M.L.H. Green, B. Jewitt, A.F. Orchard and C.F. Pygall, *J. Chem. Soc., Faraday Trans. II*, (1972) 1847.
- 41 E. Weiss and E.O. Fischer, *Z. Anorg. Allg. Chem.*, 278 (1955) 219.
- 42 E. Weiss and E.O. Fischer, *Z. Anorg. Allg. Chem.*, 284 (1956) 69.
- 43 A. Almenningen, A. Haaland and T. Motzfeld, *Selected Topics in Structural Chemistry*, Universitetsforlaget, Oslo, 1967.
- 44 L. Hedberg and K. Hedberg, *J. Chem. Phys.*, 53 (1970) 1228.